ISSN 2989-0705 (Online)|Vol 3|Issue 1|January 2025

Green Synthesis of Silver Nanoparticles using the leaf extracts of Ginger family plants (*Zingiberaceae*) for enhanced antioxidant, antimicrobial, and photocatalytic activity.

Fathima Rizvi[1] and Mathivathani Kandiah[1*]

[1]School of Management, Business Management School (BMS), Sri Lanka

*mathi@bms.ac.lk

Abstract

Nanoscience is an expanding research field impacting nearly all the branches of science. The synthesis of metal nanoparticles is a growing field of study due to its potential to be used in the creation of novel technologies. Silver is used to synthesize nanoparticles because of their unique properties, such as shape and size-dependent optical, electrical, and magnetic characteristics. The primary objective of this research was to analyze the antioxidant, antimicrobial and photocatalytic activity of silver nanoparticles (AgNPs) synthesized using leaf extracts from ginger family plants. Changes in color and characterization by UV-Vis spectrophotometer and scanning electron microscopy (SEM) were used to confirm the synthesis of AgNPs. According to the SEM analysis, the AgNPs were spherical in shape and 40- 50 nm in size. Total Antioxidant Capacity (TAC), Total Flavonoid Content (TFC), Total Phenolic Content (TPC), DPPH (2,2-diphenyl-1-picrylhydrazyl), and inhibitory concentration50 (IC50) assays confirmed a significant difference ($P< 0.05$) in the presence of higher amounts of antioxidants in AgNPs compared to aqueous extracts of the leaves. The antimicrobial activity of the synthesized AgNPs were detected using *Escherichia coli* and *Staphylococcus aureus*, using well-diffusion technique. However, no significant difference was observed between AgNps and bacterias as ginger species too have antimicrobial activity. Out of all the photocatalytic activity, AgNP *Zingiber officinale* (ZO) was evaluated at concentrations of 267 ppm and 4000 ppm in the presence of $NaBH_4$ under sunlight, showed that Erichrome Black-T (EBT) degraded within 80 minutes at 267 ppm and within 65 minutes at 4000 ppm, as indicated by the reduction of the peak at 520 nm. Furthermore, the rate constant for the degradation were 0.0265 for 267 ppm and 0.0337 for 4000 ppm AgNP ZO, demonstrating that EBT degraded faster at the higher concentration. Therefore, AgNPs synthesized in this work have the potential for versatile applications which require antioxidant, anti-microbial or catalytic activity.

Keywords: Nanoparticles, Green synthesis, *Zingiberaceae*, Antimicrobial activity, Antioxidant

1. Introduction

Nanoscience and nanotechnology are expanding research fields that involve structures, devices, and systems with novel properties and functions because of the arrangement of their atoms on the 1–100 nm scale.

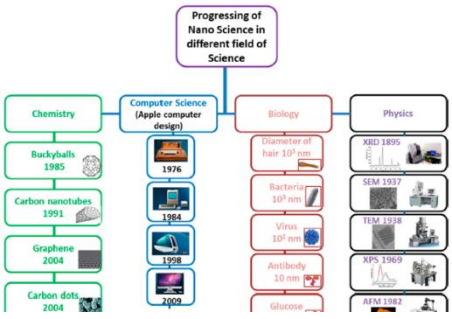

Figure 1. Progress in nanoscience and nanotechnology in different field of science.[1]

In the early 2000s, there was a growing public awareness and controversy about the field, which led to the beginning of commercial applications of nanotechnology. Nanotechnologies have an impact on nearly every branch of science, including physics, materials science, chemistry, biology, computer science, and engineering (Figure1).[1]

In 1959, American physicist Richard Feynman proposed the concept of nanotechnology thus he is regarded as the father of modern nanotechnology. Later, Norio Taniguchi, a Japanese scientist, was the first to use and define the term "nanotechnology" in 1974 as "the processing of separation, consolidation, and deformation of materials by one atom or one molecule".[1,2]

Metal nanoparticles have found wide acceptance because of their unique chemical and physical properties, higher reactivity, different shape, nondispersive size, and particularly optical properties like surface plasmon resonance (SPR).[3] AgNPs are the most thoroughly researched nanoparticles as they have immense broad-spectrum activities. AgNP research has made significant advances in nanoscience, particularly as antimicrobial, antibacterial, antioxidants, antifungal, anti-inflammatory, anticancer, and anti-angiogenic agents (Figure 2). AgNPs are small particles with unique physicochemical properties, ranging in size from 10 to 100 nm (size, shape, optical activity, electric conductivity, high surface area).[4,5]

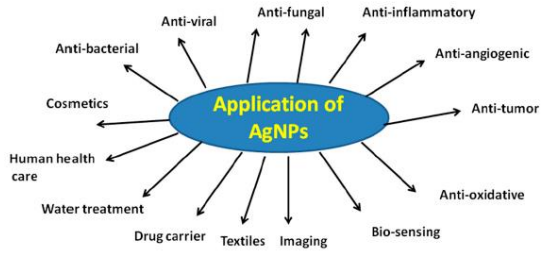

Figure 2. Various applications of AgNPs.[6]

To meet the demand for AgNPs, a variety of synthesis methods have been used such as top down and bottom methods (Figure 3). Physical and chemical techniques are widely used, but physical techniques are unaffordable; chemical techniques, on the other hand, are hazardous to the environment and living organisms. Biologically prepared AgNPs, on the other hand, have a high yield, solubility, and stability.[2] Biological methods appear to be simple, rapid, non-toxic, dependable, and green approaches for producing well-defined size and morphology under optimized conditions for translational research among several synthetic methods for AgNPs. Bio-inspired approaches based on natural products such as micro- or marine organisms, proteins, and plant extracts (PEs) have gained popularity for the synthesis of AgNPs. The cost of microbe-mediated synthesis, followed by extracellular and intracellular mechanisms, is high, and there is a risk of contamination in the microbial culture. Thus, plant extracts have received much interest because they are simple to use, cost effective and more tolerant to metal toxicity.[4,7]

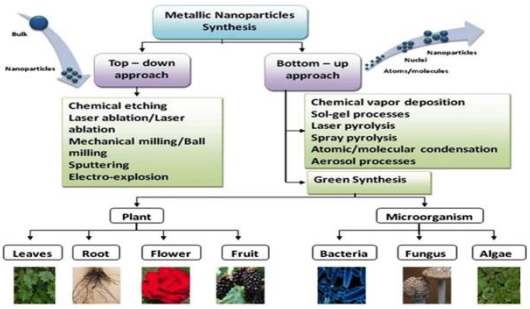

Figure 3. Types of metallic nanoparticle synthesis.[8]

Plant parts such as the leaf, stem, seed, fruit, pulp, peel, flower, and plant nectar (honey) provide a better platform to produce specific phytochemicals for the fabrication of AgNPs.[3] In this study, we used green synthesis method (Figure 4) to synthesize silver nanoparticles using leaf extract of *Zingiberaceae* species which act as a reducing and stabilizing agent. Ginger's pungent aroma comes from its volatile oil, gingerol, and other active components. These bioactive ginger constituents are known to inhibit prostaglandin and leukotriene formation by regulating blood flow, as well as to control inflammation. Ginger, on the other hand, has moderate antioxidant properties against a variety of bacterial strains.[4,9] Ginger's pharmacological activities as antifungal, antibacterial, anti-inflammatory, and antioxidant properties were primarily attributed to its active phytocompounds such as, 6-gingerol, 6-shogaol, and zingerone, in addition to other phenolics and flavonoids.[10,11]

Antioxidants are defined as "any chemical that delays, prevents, or eliminates oxidative damage to a target molecule" and are thought to be crucial to the body's defensive system against reactive oxygen species (ROS).[12]Antioxidants have a variety of physiological functions in the body because they block the process of oxidation even at low concentrations. Radical scavengers such as the antioxidant components of plant material serve to reduce the reactivity of radicals. Fruits, vegetables, tea, and other dietary sources include a variety of antioxidants that can scavenge free radicals.[13,14]

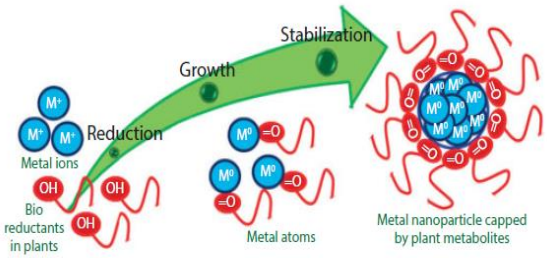

Figure 4. Green synthesis mechanism.[2]

The use of antioxidants protects the human body from cardiovascular, neurological, and carcinogenic diseases, as well as delaying chronic health problems such as cataracts.[14]

Silver has been shown to be highly toxic to a wide variety of microorganisms. Silver ions are antibacterial because they interact with the peptidoglycan cell wall and plasma membrane, and they also prevent bacterial DNA replication.[15] AgNPs' antibacterial activity is determined by the concentration of nanoparticles exposed to bacteria as well as the type of bacteria.[7]

Smaller nanoparticles have greater antibacterial activity because they have more surface exposure to the bacterial membrane. The positive charge of Ag+ interacts with the negative charge on the cell wall of bacteria, causing changes in cell wall morphology and an increase in cell permeability or leakage, resulting in cell death (Figure 5).[16]

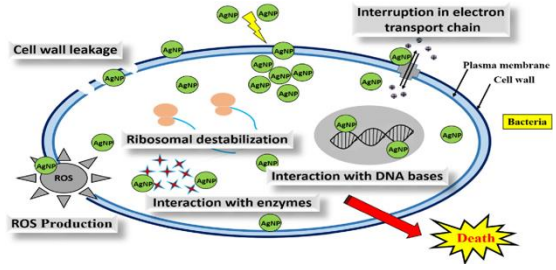

Figure 5. Mechanisms of antimicrobial activity for AgNPs .[16]

Since industrial pollutants are made up of various dyes (Figure 6) that are chemically stable, removing synthetic dyes from wastewater is a serious environmental issue that must be tackled scientifically. AgNPs are known to absorb light in the visible range of the light spectrum due to its Surface plasmon resonance characteristics. The photocatalytic nature of AgNPs is determined by the crystallographic nature, morphological structure, and size of the nanoparticles. Under ambient temperature and visible light illumination, AgNPs are highly efficient, and stable photocatalysts.[17] Degradation techniques are one of the beneficial processes that have been applied for dye removal from wastewater and pharmaceutical industries among various chemical and physical methods.[18]

Hence the aim of this study was to analyse the antimicrobial and antioxidant activity of silver nanoparticles synthesized using leaf extracts of five varieties of ginger species. The antioxidant properties were assessed by TFC, TPC, and TAC. *Escherichia coli and Staphylococcus aureus* was used to detect the antimicrobial activity performing well diffusion technique. The photocatalytic activity was assessed by using EBT dye. Thus, these AgNPs could be used in various field for the betterment of world.

Figure 6. Example for Azo dye.[18]

2. Methodology

2.1. Sample Collection. Leaves from five different species (Fig 7) of ginger family plants were collected from a plant nursery in Battaramulla.

2.2 Preparation of leaf extracts using distilled water: the samples were air-dried and ground into smaller pieces. Two grams of each ground sample were mixed with 40 mL of distilled water. The samples were incubated at 60°C for 15 min, then filtered into falcon tubes and stored at 4°C for future use.

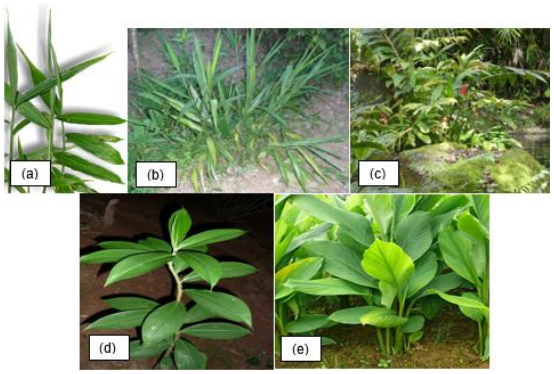

Figure 7. Varieties of ginger species used to synthesize nanoparticles*:* a) *Zingiber officinale - ZO (Ginger)* b) *Alpinia calcarata- AC (Snap ginger)* c*) Zingiber zerumbet- ZZ (Pinecone ginger)* d*) Costus speciosus- CS(Thebu)* e) *Carcumo longa- CL*

2.3 Green Synthesis of AgNPs and optimization. One milliliter of each water extract was mixed with 9 mL of 1 mM $AgNO_3$ solution and left at room temperature for 24 hours. Optimization was conducted at both 90°C and 60°C temperatures for durations of 15 min, 30 min, 45 min, and 60 min respectively. The color change of the samples was observed, and the absorbance was measured from 320 to 500 nm, using distilled water as a blank for all conditions.[19]

2.4. Dilution of the samples. AgNPs and the water extracts were diluted with a dilution factor of 1:15 and were stored at 4°C for further use.

2.5. Phytochemical Tests. The phytochemical analysis was conducted according to the methodologies shown below in Table 1.

2.6. Determination of Total Flavonoid Content. TFC was determined using $AlCl_3$ solution. For that, 1.5 mL of the sample was mixed with 1.5 mL of 2% $AlCl_3 \cdot 6H_2O$ solution and incubated at room temperature (RT) for 10 mins. The absorbance of the samples was measured at 415 nm using distilled water as the blank. Three replicates were conducted for each sample. The TFC was expressed as quercetin (mg/g) to construct the calibration curve.[11]

2.7 Determination of Total Antioxidant Activity: The phosphomolybdenum reagent was prepared by mixing equal volumes of 28 mM sodium sulphate and 4 mM ammonium molybdate and 0.6 M sulphuric acid (1:1:1). Exactly, 3 mL of the sample was mixed with 1 mL of the phosphomolybdenum reagent, and incubated at 90 °C for 90 min. The absorbance was measured at 695 nm in triplicates, using distilled water as a blank. Final concentration TAA was expressed as ascorbic acid equivalence (mg AAE/100g).[22]

Table 1. Phytochemical tests and the methodology.[20,21]

Phytochemical Test	Methodology
Carbohydrate	To 0.5 mL of sample, 1 mL of Molisch's reagent was added along with few drops of Conc. H_2SO_4
Amino Acid	Few drops of Ninhydrin solution were added to 0.5 mL sample and was kept in water bath for 10 mins
Saponins	To 0.5 mL of sample, 0.5 mL of distilled water was added and shaken vigorously for 10 mins
Tannins	To 0.5 mL of sample, 1 mL of 5% ferric chloride was added.
Proteins	To 0.5 mL of sample, few drops of Millon's reagent was added.
Terpenoids	To 0.5 mL of sample, 0.5 mL of chloroform along with few drops of Conc. H_2SO_4 was added.
Quinones	To 0.5 mL of sample, 0.5 mL of Conc. H_2SO_4 was added
Betacyanin	To 0.5 mL of sample, 0.25 mL of 2M NaOH was added and heated for 5 mins at 100◦C

2.8. Determination of Total Phenolic Content. Exactly, 0.5 mL of the sample was mixed with 2 mL of 7.5 % Na_2CO_3 and 2.5 mL of Folin–Ciocalteu reagent diluted with water in 1:10 v/v ratio. The mixture was incubated at 40 °C for 30 mins. The absorbance was measured at 765 nm in triplicates, using distilled water as a blank. The TPC was expressed as gallic acid equivalents (mg GAE/100g).[11]

2.9. Determination of Antimicrobial Activity. The antimicrobial activity was determined using two types of bacterial strains *Staphylococcus aureus* and *Escherichia coli* using the agar well-diffusion technique on Mueller-Hinton agar.The bacterial culture was evenly spread on MHA plates using a cotton swab. Three wells were created on the plates for the negative control (−) and two sample replicates (S1 and S2), as shown in Figure 8. Exactly, 1 mL of saline solution was added to the negative control, and 1 mL of the sample was added to each S1 and S2. Gentamycin discs were used as the positive control (+). The plates were incubated at 37°C for 24 hours and the

zone of inhibition diameter was measured using a ruler.[19]

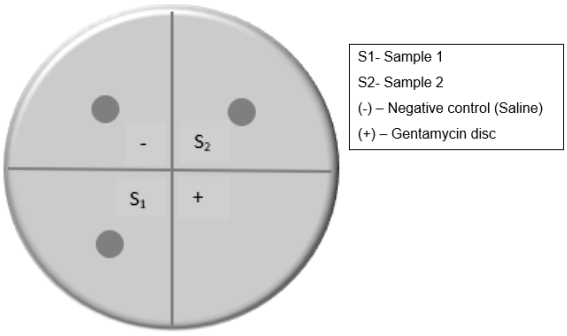

Figure 8. Labelled petri dish for antimicrobial activity.

2.10. Photocatalytic Activity. Exactly, 1 mL of 4,000 ppm of Zinc Oxide Silver Nanoparticles (ZO AgNPs) and 1 mL of 0.2M $NaBH_4$ were added to 100 mL of 1 mM EBT. A 0.5 mL aliquot of the mixture was diluted to 3 mL with distilled water, and the absorbance was measured in the range of 320 to 800 nm every 10 minutes over a period of 80 minutes, using distilled water as the blank. The same procedure was repeated for 267 ppm ZO AgNPs.[19]

2.11. DPPH assay. Exactly, 2 mL of 0.004% DPPH was mixed with 1 mL of sample and incubated for 30 mins at RT. The absorbance was measured at 517 nm in triplicates, using methanol as a blank. The following equation was used to calculate the %DPPH activity.[23]

$$\% \text{ activity} = \{(A_{(sample)} - A_{(control)})/ A_{(control)}\} \times 100$$

2.12. Determination of Median Inhibitory concentrations (IC50). Exactly, 2 mL of 0.004% DPPH was added to 1 mL of each sample and then a dilution series was prepared with concentrations of 100 %, 80 %, 60 %, 40 %, and 20 % respectively. and was incubated for 30 mins at RT. The absorbance was measured at 517 nm using methanol as a blank. The % DPPH was calculated using the same equation of DPPH assay.[23]

2.13. SEM analysis. The ZO sample was sent to Sri Lanka Institute of Nanotechnology (SLINTEC) for SEM analysis using Hitachi SU6600 SEM.

2.14. Statistical Analysis: ONE-way ANOVA test and correlation graphs were generated using the Microsoft 365 data analysis and SPSS software, respectively.

3. Results

3.1 Phytochemical Tests.

Based on the phytochemical tests conducted (Table 2), all Zingiber species contain carbohydrates and quinones.

Table 2. Results of phytochemical tests.

Phytochemical Test	CS	CL	AC	ZO	ZZ
Carbohydrate	✓	✓	✓	✓	✓
Amino Acid	✗	✗	✓	✗	✓
Saponin	✗	✗	✗	✗	✗
Tannins	✗	✓	✗	✓	✗
Proteins	✓	✗	✓	✗	✓
Terpenoids	✗	✗	✗	✓	✗
Quinones	✓	✓	✓	✓	✓
Betacyanin	✓	✓	✓	✗	✗

3.2 Synthesis of AgNPs from Zingiberaceae species.

The samples changed their color (Figure 9) to shades of yellow from colourless, indicating the synthesis of AgNPs due to reduction of Ag+ to Ag. This is further proved by spectrophotometer analysis as there was a clear peak formation from 400 nm to 480 nm in samples CL, ZO, and ZZ at 90◦C for 60 mins.

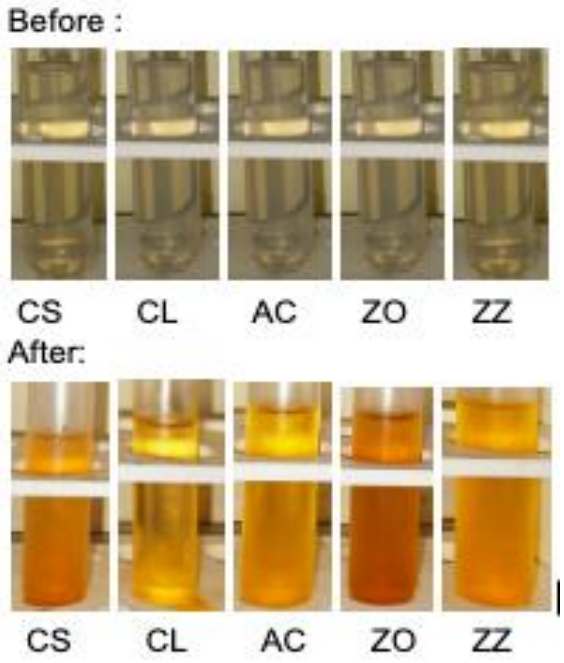

Figure 9. Synthesis of AgNPs from *Zingiberaceae* species at 90◦C for 1 hour.

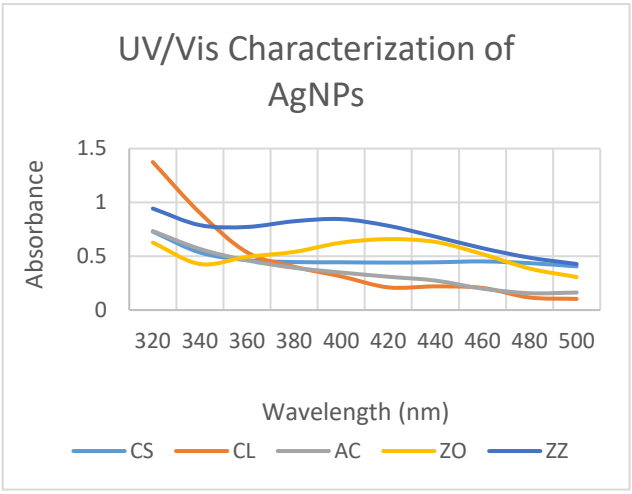

Figure 10. UV-Spectrophotometer analysis of

3.3 SEM Analysis.

According to SEM analysis the AgNPs were spherical in shape and 10 nm in size (Figure 11).

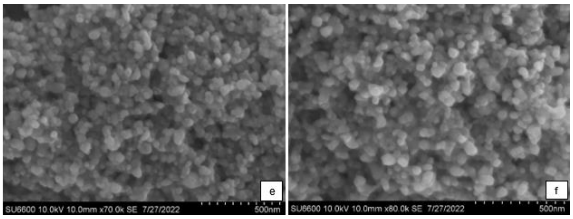

Figure 11. Electron microscopy at 500 nm.

Table 3. Optimization temperature of AgNPs

	90◦C				60◦C				25 ◦ C
	Time (mins)				Time (mins)				
Sample ID	15	30	45	60	15	30	45	60	
CS	✗	✗	✗	✗	✓	✗	✗	✗	✗
CL	✗	✗	✗	✓	✗	✓	✗	✗	✗
AC	✗	✗	✗	✗	✗	✓	✗	✗	✗
ZO	✓	✓	✓	✓	✓	✓	✓	✓	✗
ZZ	✗	✓	✓	✓	✓	✗	✓	✓	✗

3.4 Total Flavonoid Content.

TFC of AgNPs is higher than that of the water extract (Figure 12). Thus, this was further proved by the One-way ANOVA test, which showed a significance difference (P< 0.05) of (P= 0.00359) between water extract and AgNPs.

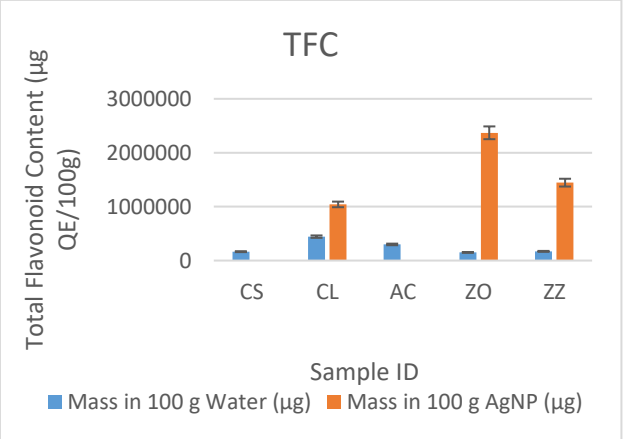

Figure 12. TFC of *Zingiber* species water extract and AgNPs.

3.5 Total Phenol Content.

TPC is comparatively higher in AgNPs than that of the water extract (Figure 13). One-way ANOVA analysis also showed a significance difference (P<.0.05) of 7.63E-08 between water extract and AgNPs.

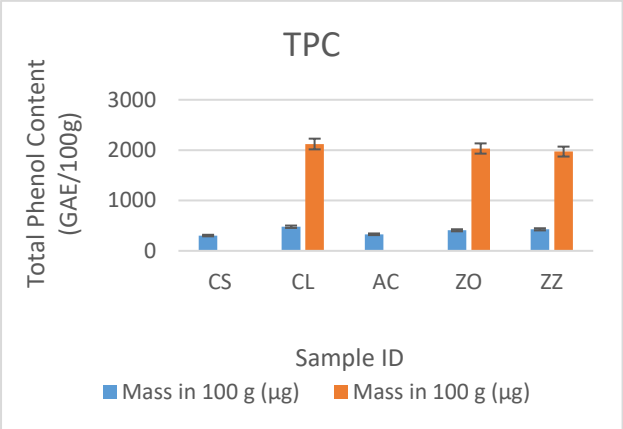

Figure 13. TPC of Zingiber species water extract and AgNPs.

3.6 Total Antioxidant Capacity.

AgNPs have comparatively higher amounts of TAC than water extracts (Figure 14) with a significance difference of 5.32E-06. AgNP ZO has the highest TAC.

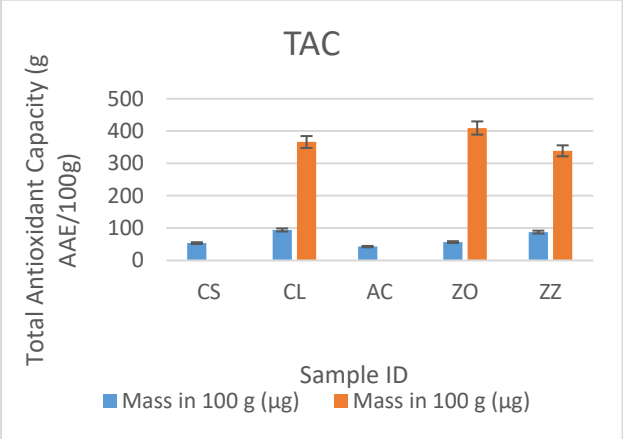

Figure 14. TAC of *Zingiber* species water extract and AgNPs.

3.7 DPPH assay.

AgNPs have higher DPPH activity compared to water extract by a minute difference (Figure 15).

3.8 IC_{50} of DPPH.

AgNPs have more antioxidants compared to water extract, as the IC_{50} value (Figure 16) is less in AgNPs than water extract (Table 4)

Table 4. IC50 of water extract and AgNPs.

Sample	Water	AgNPs
CS	11.39238	
CL	3.26094	2.949853
AC	6.122424	
ZO	4.799846	3.885004
ZZ	5.59009	3.854456

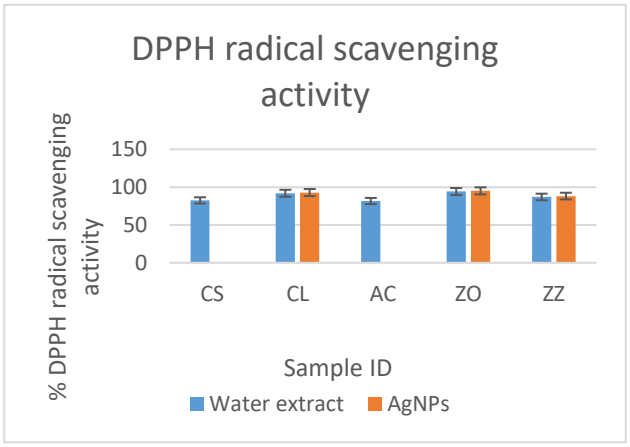

Figure 15. % DPPH radical scavenging activity for Water extract and AgNPs.

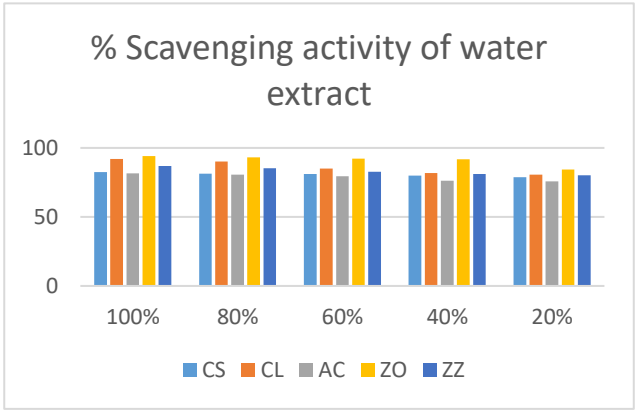

Figure 16. % Scavenging activity of AgNPs.

3.9 Photocatalytic activity of AgNP.

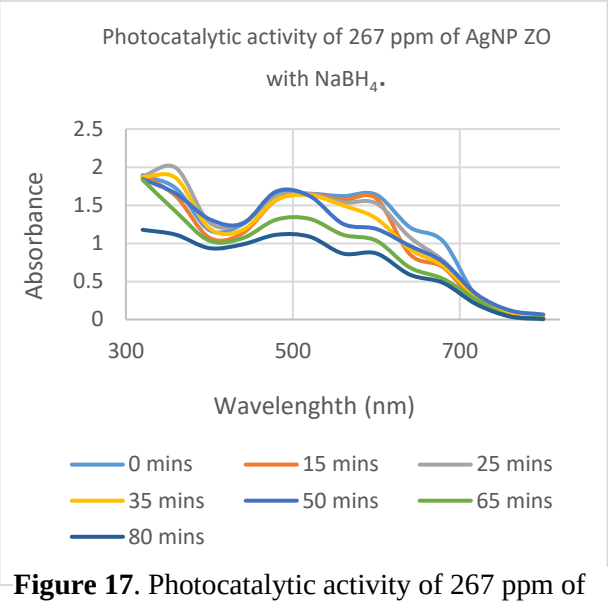

Figure 17. Photocatalytic activity of 267 ppm of AgNP ZO with $NaBH_4$ under sunlight.

EBT was degraded by 267 ppm AgNP ZO completely at 80 mins indicated by peak 520. Degradation of EBT was completed by 4000 ppm AgNP ZO at 65 mins indicated by peak 520 nm (Figure 17, 18).

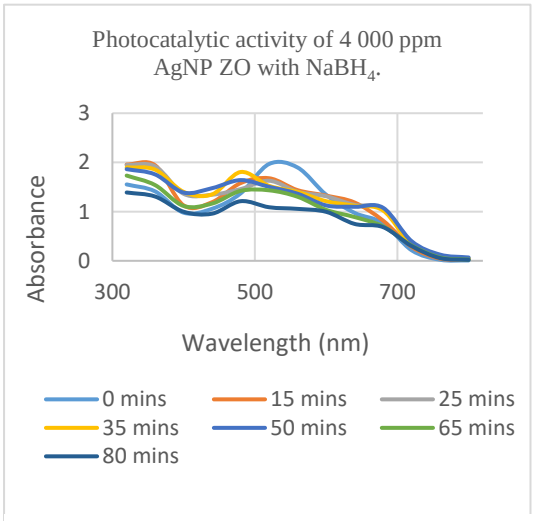

Figure 18. Photocatalytic activity of 4000 ppm AgNP ZO with $NaBH_4$ under sunlight.

3.10 Antimicrobial Activity.

ZOI of AgNP ZO and ZZ were higher than water extract (Figure 19) for *E. coli*. There was no significance (P> 0.05, P= 0.543) observed between the water extract and the AgNPs.

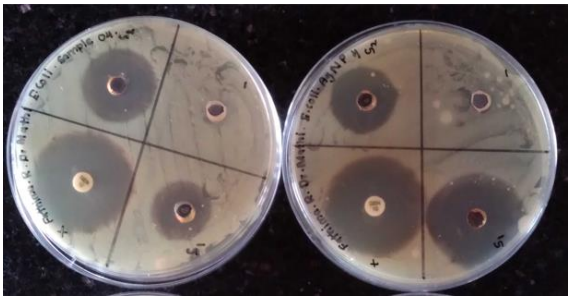

Figure 19. ZOI for *E. coli* in water extract (Left) and AgNPs (Right).

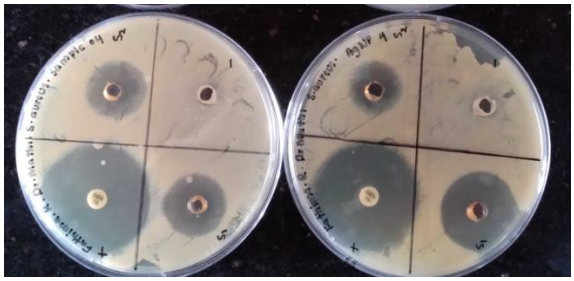

Figure 20. ZOI for *S. aureus* in water extract (Left) and AgNPs (Right).

AgNP CL and ZZ has higher ZOI compared to water extract (Figure 20) for *S. aureus*. There was no significance (0.713) seen between water extract and AgNP.

4. Discussion.

Nanoparticles with a variety of shapes, sizes, and morphologies can be synthesized using a method that is ecologically friendly, nontoxic, and reasonably priced using plant extracts. Compared to several physicochemical approaches used in production, the biosynthetic route can yield metal nanoparticles in better sizes and forms. Instead of employing microorganisms, plant extract-based nanoparticle synthesis has the benefit of not requiring multistep or complicated processes including microorganism isolation, identification, growth optimization, culture preparation, and maintenance.[16,24] In addition, plant-based synthesis is quicker than employing microorganisms, and simple to scale up for mass production of nanoparticles.[15]

Green leaves are used and preferred over other parts of plants to produce AgNPs due to their origin in photosynthesis and the availability of more Hp ions, which reduces the formation of $AlCl_3$ within the AgNPs.[7]

The extract's water-soluble components are what produces the reduction and stability of AgNPs. Thus, water was used solvent as it is less toxic and will increase the yield.[9]

Table 5. Conductivity of AgNPs.

Sample	Band Gap Energy (eV)	Classification
CS	4.32	Insulators
CL	4.51	Insulators
AC	4.73	Insulators
ZO	4.51	Insulators
ZZ	4.97	Insulators

$$E = hc \div \lambda$$

E= Band gap energy

h= Planck's Constant (6.6269×10^{-34} Js).

c= Speed of light (3×10^{8} ms^{-1}).

λ= Wavelength (400- 480 nm).

Figure 21. Planck's Equation.

It was obvious that AgNPs had formed in the reaction mixture during the early stages of reduction because the colour changed from nearly colourless to brown and due to clear peak formation from 400 to 480 nm in UV-Vis spectrophotometer analysis. With time during incubation, the colour intensity increased. The dark brown colour of the yellow solution over time may be related to both the increased concentration of AgNPs and the reduction in particle size.[25] The change of colour may be due surface plasmon resonance of AgNPs caused by an interacting electromagnetic field, the collective oscillation of free conduction electrons. The SEM analysis indicated that the AgNPs had a spherical structure with 40 nm size (Figure 11). Similar research has proven that AgNPs synthesized using ginger extract was spherical particles and polydisperse with size ranging from 3-6 nm.[24,25,26] The obtained results show that under reaction conditions, ginger leaves extract had reduced Ag+ to Ag0.[15]

One of the widely used techniques for characterizing particles and their properties is UV-Vis spectroscopy. The bandgap caused by electron transitions between the top of the valence band and the bottom of the conduction band, was used to investigate the conductivity of AgNPs. Materials can be categorized as insulators or semiconductors depending on whether the lowest energy needed for an electron transition is more than 4eV or less than 3eV respectively.[22] Accordingly, the bandgap energy of *Zingiberaceae* AgNPs was measured using the Plank's Equation (Figure 21) and it was between 4.30 and 4.98 and thus, considered as insulators (Table 5).

Ginger consists of various bioactive components, like phenolic and terpene. Gingerols, shogaols, and paradols are the primary phenolic chemicals found in ginger. Thus, it was proved by the phytochemical screening assays (Table 2).[27]

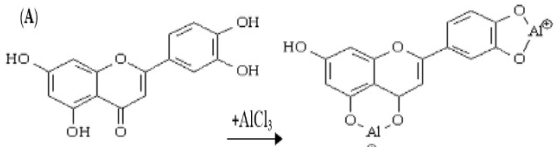

Figure 22. Total Flavonoid Content Principle.[29]

Overproduction of free radicals, such as ROS, is known to play a significant role in the development of many chronic diseases. Numerous natural products, including vegetables, fruits, edible flowers, cereal grains, medicinal plants, and herbal infusions, have been documented to have antioxidant potential. Numerous studies have revealed that ginger has a significant antioxidant capacity.[27]

TFC was measured using the $AlCl_3$ colorimetric approach. The fundamental idea behind the assay is that AlCl3 forms acid-stable complexes with flavones and flavanol C-4 keto groups as well as either C-3 or C-5 hydroxyl groups (Figure 22). Additionally, it combines with the ortho-dihydroxyl groups on the A or B ring of flavonoids to generate complexes that are acid labile.[28,29] According to this study, AgNPs (ZO> ZZ> CL) has higher amount of TFC

compared to water-extract. ONE-way ANOVA test further supported the study by showing a significance of 0.0024 (<0.05) between AgNPs and water-extract. In addition, a study has proved that AgNPs synthesized from the rhizome of ginger has more TFC than the water-extract.[30]

The most used colorimetric assay for phenolic content is Folin-Ciocalteu (F-C) assay. The F-C reagent is composed of a tungsten and molybdate combination. The phosphomolybdic acid complexes are formed when phenolic chemicals transfer electrons to them under alkaline conditions. The quantity of reactive phenolic chemicals in the sample directly correlates with the intensity of the blue colour. By measuring the sample solution's absorbance at 765 nm and comparing it to a calibration curve using gallic acid as a standard, the phenol concentration is determined. The coordinated molybdenum(V) species is assumed to be the cause of the blue colour that results from the reduction of the F-C reagent (Figure 23).[31,32] Hence, TPC was comparatively higher in AgNPs (CL> ZO> ZZ) than the water-extract. It was further proved by ONE-way ANOVA analysis which showed a significance of 7.63E-08 (<0.05) between water-extract and AgNPs. Based on the research by Jaiswal and Naik (2018), AgNPs synthesized from the rhizome of ginger has more TPC compared to water-extract.

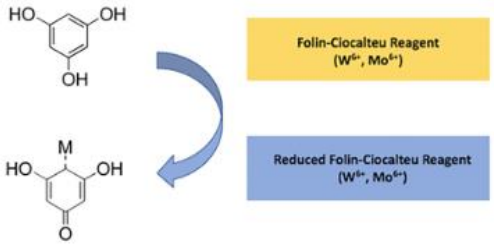

Figure 23. Total Phenol content Principle.[32]

When Mo (VI) is reduced to Mo (V) at an acidic pH, antioxidants produce a green phosphate/Mo (V) complex, which can be detected at 695 nm. This complex is used to determine TAC.[22] Thus, synthesized AgNPs (ZO> CL> ZZ) has comparatively higher amount of TAC than water-extract. In addition, it was validated by ONE-way ANOVA test between water-extract and AgNPs with a significance of 5.32E-06.

DPPH has been frequently used to assess how well different antioxidant compounds scavenge free radicals. Antioxidants can donate hydrogen in the DPPH assay, reducing the stable radical DPPH to the yellow nonradical diphenyl-picrylhydrazine (DPPH-H) (Figure 24). Based on the spectrophotometric measurement of the change in DPPH absorption at 517 nm, and a deep violet colour results from the electron's delocalization. DPPH is typically employed as a reagent to assess the free radical scavenging activity of antioxidants.[33] Methanol or ethanol is employed in the DPPH assay to maintain the hydrophobic hydroxyl radicals and phenolic test chemicals in solution while providing adequate buffering capacity.[22]

AgNPs (ZO> CL> ZZ) has a higher %DPPH activity compared to water-extract which corresponds to the result of TAC. Moreover, it has been proved in a study that AgNPs synthesized using the callus of ginger has comparatively higher %DPPH activity than water-extracts.[11]

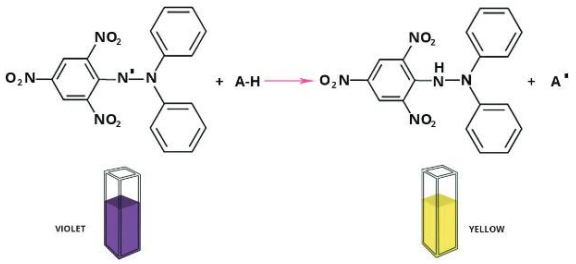

Figure 24. DPPH Assay.[10]

Low IC_{50} value values indicate strong antioxidant activity, and the reaction is preceded by a rapid drop in absorption.[34] So, it can be concluded AgNPs have a higher antioxidant activity than water-extract.

Pearson Correlation factor for all the antioxidant assays were higher than 0.8 (Figure 25). Hence it proves the correlation between all three assays.

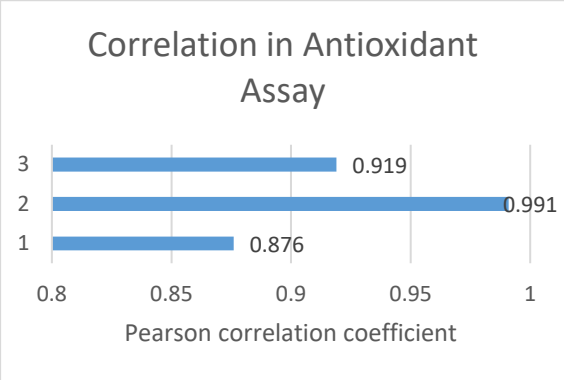

Figure 25. Pearson correlation for the antioxidant assays.

The surface electrons from the outermost sp band are excited to a higher energy state as a result of the SPR effect when AgNPs absorb visible light from the solar spectrum; these electrons are quickly accepted by the O_2 molecules to form oxygen radicals that attack and degrade the EBT. Additionally, the dye is degraded as a result of accepting electrons from the adsorbed photosensitized dye molecule to fill the holes created in the 5sp orbital.[17] Numerous photogenerated electrons are excited as a result of inter-band transition. Both oxygen radicals and hydroxyl radicals are created when these excited electrons interact with O_2 molecules and hydroxyl ions respectively. The dye is degraded as a result of the radicals' attack on the dye molecule adsorbed on the surface of the AgNPs.

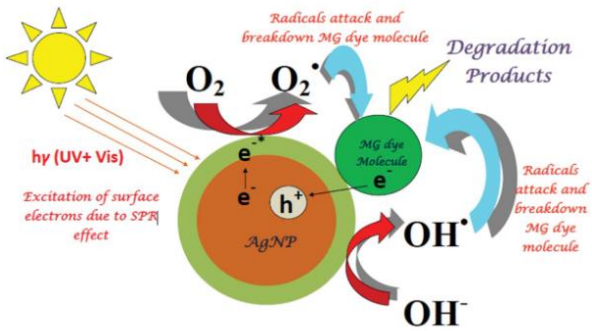

Figure 26. Photocatalytic activity of AgNPs.[17]

In addition to the radicals degrading the dyes, the holes made in the AgNPs' d orbital take electrons from the dye that has been adsorbed, further degrading the dye (Figure 26).[17,18]

While the absorbance of the dye reduces just slightly in the absence of the catalyst, suggesting a relatively slow reaction rate, it abruptly decreases in the presence of the catalyst, indicating a faster reaction rate. As an electron relay, AgNPs start the process of moving an electron from a BH_4^- to an acceptor, which reduces the dye. NPs are simultaneously adsorbed with the BH_4-, allowing for the transfer of electrons from the BH_4- to the dye.[35]

In this study, the photocatalytic activity of AgNP ZO under sunlight and UV-light without catalyst didn't show any degradation. So, the study was done using catalyst $NaBH_4$ under sunlight to degrade EBT dye. It was observed that the EBT degraded within 65 and 80 mins by 267 and 4000 ppm AgNP ZO respectively indicated by peak 520 nm. This was further justified by calculating the photocatalytic rate constant using the equation in Figure 27. 4000 ppm AgNP ZO had a higher rate constant of 0.0337 (Figure 28) than 267 AgNP (k= 0.0265) (Figure 29).

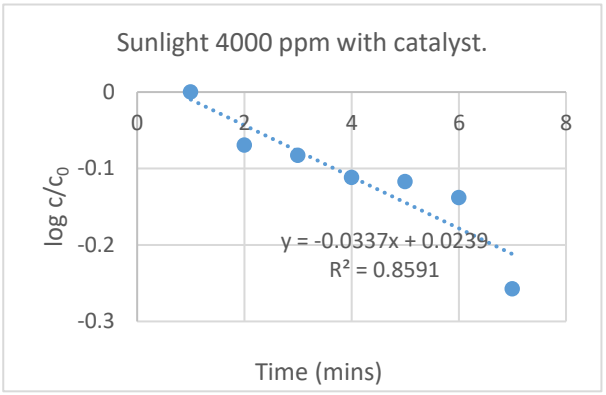

$$log\ c/c0\ =\ -kt$$

c= Concentration

c0= Concentration at 0 mins

k= Rate constant

t= Time

Figure 28. Rate constant of 4000 ppm AgNP.

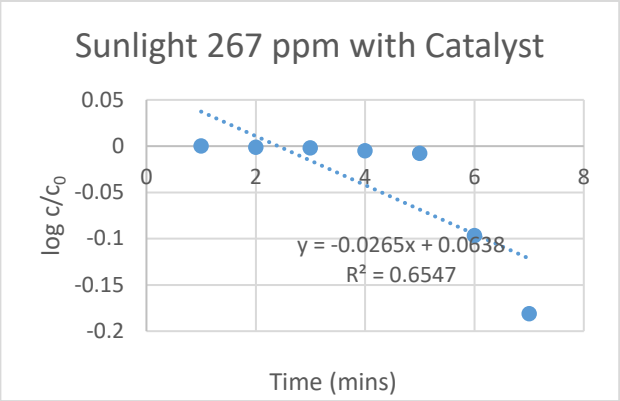

Figure 29. Rate constant of 267 ppm AgNP.

Numerous studies have detailed the use of AgNPs in a broad range of antimicrobial applications, including the treatment of wounds and the combating of clinical isolates, nosocomial, and food pathogens. The concentration of nanoparticles exposed to bacteria and the type of bacteria affect AgNPs' antibacterial activity. AgNPs have different bactericidal activities against gram-positive and gram-negative bacteria, however it is possible to distinguish which is more effective. Gram-negative bacteria are discovered to be more sensitive to AgNPs than gram-positive bacteria, according to certain research findings; nevertheless, other researchers found the opposite to be true. [16,35]

Due to their increased surface exposure to the bacterial membrane, the smaller nanoparticles exhibit more antibacterial action. It is thought that silver interacts with the thiol groups of proteins on cell membranes, preventing respiration and ultimately leading to death. (Figure 5).[16]

According to the current study it was observed that AgNP ZO and ZZ had a higher ZOI in *E. coli* than water extract; whereas AgNP CL had a less ZOI compared to the water extract. This may be due to the presence of antimicrobial activity present in ginger family. Moreover, ONE-way ANOVA didn't show significance difference (p=0.542) between AgNP and water-extract.

For *S. aureus* only AgNP CL and ZZ has higher ZOI than water extract while AgNP ZZ had a smaller ZOI. And no significant difference was observed between water-extract and AgNP (p=0.713).

In this study, it has been found more ZOI for E. *coli* than *S. aureus*. The peptidoglycan layer's different composition and thickness in the cell wall could be the most likely cause. Gram-positive bacteria have a three-dimensional peptidoglycan coating that is ~80 nm thick, which makes them less vulnerable to attack by AgNPs than Gram-negative bacteria.[36]

5. Conclusion

In conclusion, only three AgNPs (CL, ZO, and ZZ) synthesized from the leaf extracts of five species of ginger family plants exhibited spherical structures and measured 10 nm in size. All the AgNPs had higher antioxidant than water extract based on TFC, TPC, TAC, DPPH and IC_{50} assays. However, there was no significant difference between AgNPs and water-extract was observed for the anti-microbial activity of E. coli and S. aureus. Furthermore, 4000 ppm AgNP ZO degraded the EBT dye faster than 267 ppm AgNP ZO. Thus, further studies could focus on exploring microbial activity, with a particular emphasis on the potential of AgNPs for medicinal applications. Additionally, AgNPs could be utilized to help mitigate pollution caused by azo dyes, offering a promising approach to environmental remediation.

Acknowledgements

Authors would like to thank SLINTEC for allowing us to carry out the SEM analysis using Hitachi SU6600 SEM.

References

1 S. Bayda, M. Adeel, T. Tuccinardi, M. Cordani,and F. Rizzolio. *Molecules.* 2019;**25**(1);112.
2 S. Sajjad, S.A.K .Leghari, N. Ryma and S.A. Farooqi. *Green Metal Nanoparticles*. 2018;23-77.
3 M.S, Mehata. *Mater Sci Eng B*. 2021;**273**:115418.
4 A.H. Alkhathlan, H.A. AL-Abdulkarim, M. Khan, A. AlDobiy, M. Alkholief, A. Alshamsan, H.Z. Alkhathlan and M.R.H. Siddiqui. *Sustainability*. 2020;**12**(24);10523.
5 N. Jain, P. Jain, D. Rajput and U.K. Patil. *Micro Nano Syst Lett*. 2021;**9**(1).
6 X.F. Zhang, Z.G. Liu, W. Shen and S. Gurunathan. *Int J Mol Sci.* 2016;**17**(9);1534.
7 S.M. Mousavi, S.A. Hashemi, Y. Ghasemi, A. Atapour, A.M. Amani, A.D. Savar, A. Babapoor and

O. Arjmand. *Artif Cells Nanomed Biotechnol*. 2018;**46**(3);855-72.
8 J. Singh, T. Dutta, K.H. Kim, M. Rawat, P. Samddar and P. Kumar. *J Nanobiotechnol*. 2018;**16**(1).
9 K.P. Kumar and W. Paul. *BioNanoSci*. 2012;**2**(3);144-52.
10 B. Lukiati, S.S. Nugrahaningsih and R. Masita. *AIP Conf Proc*. 2020;**2294**;020015
11 A. Amma, M.E.M. El-Nour and S.M. Yagi. *J Genet Eng Biotechnol.* 2018;**16**(2);677-82.
12 B. Halliwell. *Biochem Soc Trans*. 2007;**35**(5);1147-50.
13 O. Boxin, D. Huang, M. Hampsch-Woodill, J.A. Flanagan and E.K. Deemer. *J Agric Food Chem*. 2002;**50**(11);3122-8.
14 A. Yadav, R. Kumari, A. Yadav, J.P Mishra, S. Srivatva and S. Prabha. *Res Environ Life Sci*. 2016;**9**(11);1328-31.
15 E. Abbasi, M. Milani, S.A. Fekri, M. Kouhi, A. Akbarzadeh, H.T. Nasrabadi, P. Nikasa, S.W. Joo, Y. Hanifehpour, K. Nejati-Koshk and M. Samiei. *Crit Rev Microbiol.* 2014;**42**(2);173-180.
16 M.P. Patil and G.D. Kim. *Appl Microbiol Biotechno*l. 2016;**101**(1);79-92.
17 M.B. Sumi, A. Devadiga, K.V. Shetty and M.B. Sumi. *J Exp Nanosci.* 2016;**12**(1);14-32.
18 S. Fardood, R. Forootan, F. Moradnia, Z. Afshari and A. Ramazani. *Mater Res Express*. 2020;7(1);015086.
19 B.R. Perera and M. Kandiah. *Int J Multidiscip Stud*. 2018;**5**(2);62.
20 U. Usunobun, N.P. Okolie, O.G. Anyanw and A.G. Adegbegi. *Eur J Bot Plant Sci Pathol*. 2014;**12**;18-28.
21 K.S. Banu and L. Cathrine. *Int J Adv Res Chem Sci*. 2015;**2**(4);25-32.
22 H.D.S.P.M. Abhayawardena and M. Kandiah. *GARI Int J Multidiscip Res*. 2020;**6**(5).
23 K.N. Chandrasekaran and M. Kandiah. *J Nanotechnol*. 2021;**2021**;1-18.
24 M. Reda, A. Ashames, Z. Edis, S. Bloukh, R. Bhandare and H.S. Abu. *Processes*. 2019;**7**(8);510.
25 G.H. Priya and K.B. Satyan. *J Environ Nanotechnol*. 2014;**3**(4);32-40.
26 G. Otunola, A. Afolayan, E. Ajayi and S. Odeyemi. *Pharmacogn Mag.* 2017;**13**(50);201.
27 Q.Q. Mao, X.Y. Xu, S.Y. Cao, R.Y. Gan, H. Corke, T. Beta and H.B. Li. *Foods*. 2019;**8**(6);185.
28 F. Ahmed and M. Iqbal. *Org Med Chem Int J*. 2018;**5**(4).
29 S. Sepahpour, J. Selamat, M.A Manap, A. Khatib and A.A. Razis. *Molecules.* 2018;**23**(2);402.
30 S.G. Jaiswal and S. Naik. *Open Agric*. 2018;**3**(1);326-38.
31 S. Kupina, C. Fields, M.C. Roman and S.L. Brunelle. *J AOAC Int.* 2018;**101**(5);1466-72.
32 L. Ford L, K. Theodoridou, G.N. Sheldrake and P.J. Walsh. *Phytochem Anal*. 2019;**30**(6);587-99.
33 J.M. Lü, P.H. Lin, Q. Yao and C. Chen. *J Cell Mol Med.* 2018;**14**(4);840-60.
34 N. Sánchez, R. Salas-Coronado, C.Villanueva-Cañongo and B. Hernández-Carlos. *IntechOpen*. 2019.
35 B. Paul, B. Bhuyan, D.D. Purkayastha and S.S. Dhar. *J Photochem Photobiol B Biol*. 2015;**154**;1-7.
36 M.K. Choudhary, J. Kataria, S.S. Cameotra and J. Singh. *Appl Nanosci.* 2015;**6**(1);105-11.